A simple plankton model with complex behaviour

A Simple Plankton Model with Complex Behaviour

Irene M. Moroz[1], Roger Cropp[2], and John Norbury[1]

[1] Mathematical Institute, University of Oxford, Andrew Wiles Building, ROQ, Oxford OX2 6GG,UK
(E-mail: moroz@maths.ox.ac.uk, john.norbury@lincoln.ox.ac.uk)
[2] Griffith School of Environment, Griffith University, Nathan, Queensland, 4111,Australia
(E-mail: r.cropp@griffith.edu.au)

Abstract. In this paper we extend the P_1P_2ZN model, introduced by Cropp and Norbury [5], to investigate the effects of specialist (or discriminate) and generalist (or indiscriminate) grazing (as parameterised by ρ) on a prey-prey-predator model for plankton, in the presence of a limiting nutrient. We also examine the influence of facultative and obligate omnivory on the survival of Z as a generalist predator, as we vary the linear mortality parameter σ_Z. This leads to bifurcation transition diagrams, which also include steady state stability branches for certain critical points. For specialist grazing ($\rho = 0$) the bifurcation transition diagram shows steady states, periodic and chaotic dynamics, with very small windows of periodic behaviour, as σ_Z varies, while for generalist grazing ($\rho = 1$), we only find periodic or steady state behaviours. The dynamics is interpretable in terms of facultative/obligate omnivory of Z. Results suggest that green ocean plankton code in global climate change modelling might run more stably with generalist grazing terms and careful control of grazer mortality.

Keywords: Plankton, Predator-Prey Modelling, Chaos.

1 Introduction

Plankton are organisms that cannot swim faster than ocean currents. They comprise single-cell microscopic plants called phytoplankton (diatoms and dinoflagellates) and smaller and larger grazers called zooplankton (e.g. from ciliates and copepods to krill and jelly fish), found in the upper $50m$ sunlit layers of marine ecosystems.

Using sunlight and dissolved nutrients (e.g. nitrates, phosphates, etc, carried by rivers into oceans) phytoplankton convert CO_2 from the atmosphere during photosynthesis in the upper mixed ocean surface layer, eventually drawing it down into the deep ocean. Decomposers (viruses, bacteria and fungi) capture and recycle waste products, remineralising organic nutrients into inorganic dissolved nutrients, and thus completing the nutrient recycling loop.

8^{th} *CHAOS Conference Proceedings, 26-29 May 2015, Henri Poincaré Institute, Paris France*

Phytoplankton account for about half of global synthesis of organic compounds and CO_2 [7], as well as producing half of the world's oxygen in the atmosphere via photosynthesis [3]. They are the primary food source for zooplankton. Together, these plankton form the base of the ocean's food chain, without which sharks, tuna, mackerel and other small fish would not survive. In turn, fish provide nearly 20% of total protein for humans.

Plankton may be key indicators of climate change as production depends upon water temperature and acidity, and nutrient availability. Coccolithophore phytoplankton produce dimethylsulphide and other volatile compounds, affecting cloud formation over the oceans [4]. Long term climate change could alter the plankton community structure, affecting seasonal plankton blooms, and so affect the marine food chain. Collapse or extinction of a plankton population may push the climate system across a tipping point. Indeed Falkowski [7] writes regarding the crucial role played by phytoplankton in offsetting the effects of burning fossil fuels:

'... if the phytoplankton in the upper ocean stopped pumping carbon down to the deep sea tomorrow, atmospheric levels of carbon dioxide would eventually rise by another $200 p.p.m.$ and global warming would accelerate further.'

PlankTOM5 [13], PlankTOM10 [12], and MAREMIP (MARine Ecosystem Model Inter-comparison Project [16]. See also [1]) are examples of global marine models, representing ecosystems with many different plankton functional types, developed to quantify the interactions between climate and ocean biogeochemistry, especially through CO_2. The merit of incorporating such complex ecological models into operational global climate models is questionable in the absence of a thorough understanding of the behaviours supported by such models in their own right. Our approach is to gain understanding from a study of simpler models that focus on the essential plankton interactions.

In this paper we consider a simple model of two different prey populations of phytoplankton P_1, P_2, being eaten by a population of predator zooplankton Z, where the interacting plankton populations are connected by a single limiting nutrient N. We focus on behaviour that is possible in this P_1P_2ZN model for plankton population dynamics as we vary the zooplankton mortality parameter, and as we change the zooplankton grazing function from discriminate ($\rho = 1$) to indiscriminate ($\rho = 0$) prey hunting behaviour.

2 The Plankton Model

We study the P_1P_2ZN model for plankton dynamics:

$$\dot{P_1} = P_1[\frac{\mu_1 N}{N+\kappa_1} - \frac{\phi_1 Z}{1+\epsilon_1 P_1 + \rho\epsilon_2 P_2} - \sigma_1], \tag{1}$$

$$\dot{P_2} = P_2[\frac{\mu_2 N}{N+\kappa_2} - \frac{\phi_2 Z}{1+\rho\epsilon_1 P_1 + \epsilon_2 P_2} - \sigma_2], \tag{2}$$

$$\dot{Z} = Z[\frac{\phi_1(1-\psi_1)P_1}{1+\epsilon_1 P_1 + \rho\epsilon_2 P_2} + \frac{\phi_2(1-\psi_2)P_2}{1+\rho\epsilon_1 P_1 + \epsilon_2 P_2} - \sigma_Z], \tag{3}$$

together with the nutrient N mass conservation condition:

$$\dot{N} = -\dot{P}_1 - \dot{P}_2 - \dot{Z}, \tag{4}$$

for two phytoplankton prey populations P_1 and P_2 and one zooplankton predator Z, where $P_1 + P_2 + Z + N = 1$. See [5,6] for further details.

The various parameters appearing in equations (1)-(3) (except for ρ) are explained in Table 1.

Par.	Process	Value	Reference
μ_1	Maximum rate of N uptake by P_1	1.00	Gabric *et al.* [9]
μ_2	Maximum rate of N uptake by P_2	1.15	Muller-Niklas and Herndl [15]
κ_1	Half-saturation constant for N uptake by P_1	0.25	Slagstad and Stole-Hansen [17]
κ_2	Half-saturation constant for N uptake by P_2	0.07	Billen and Becquevort [2]
ϕ_1	Z grazing rate on P_1	6.18	Hansen *et al.* [11]
ϕ_2	Z grazing rate on P_2	1.85	Gabric *et al.* [9]
ϵ_1	Half-saturation constant for Z uptake of P_1	5.50	Fenchel [8]
ϵ_2	Half-saturation constant for Z uptake of P_2	5.50	Fenchel [8]
σ_1	P_1 specific mortality rate	0.00	Gabric *et al.* [10]
σ_2	P_2 specific mortality rate	0.26	Moloney *et al.* [14]
σ_Z	Z specific mortality rate	0.19	Moloney *et al.* [14]
ψ_1	Proportion of P_1 uptake excreted by Z	0.40	Moloney *et al.* [14]
ψ_2	Proportion of P_2 uptake excreted by Z	0.40	Moloney *et al.* [14]

Table 1. Measured parameter values for eqns (1)-(3) and their physical interpretations.

2.1 The Four Cases of Interest

There are four combinations of cases that are of interest:

- specialist (or discriminate) vs generalist (or indiscriminate) grazing;
- facultative vs obligate omnivory by Z.

The **specialist** predator ($\rho = 0$) feeds on multiple prey resources, but on each independently of the other, and in a discriminating manner. The feeding of the **generalist** predator ($\rho = 1$) on each prey resource is indiscriminate. See Cropp *et al.* [6] for a more detailed explanation of these grazing functions, which are used in the green ocean components of several climate change programs (for example by [16]).

We define Z to be a **facultative omnivore** if it can survive on either P_1 or P_2 independently:

$$0 < \sigma_Z < \min\left(\frac{\phi_1(1-\psi_1)}{1+\epsilon_1}, \frac{\phi_2(1-\psi_2)}{1+\epsilon_2}\right) = \sigma_{Zmin}, \tag{5}$$

while Z is an **obligate omnivore** if it must have P_1 present (this choice comes from the parameter values given in Table 1) in order to survive; we order P_1 and P_2 to get:

$$\sigma_{Zmin} < \sigma_Z < \max(\frac{\phi_1(1-\psi_1)}{1+\epsilon_1}, \frac{\phi_2(1-\psi_2)}{1+\epsilon_2}) = \sigma_{Zmax}. \tag{6}$$

Using the parameter values in Table 1,

$$(\frac{\phi_1(1-\psi_1)}{1+\epsilon_1}, \frac{\phi_2(1-\psi_2)}{1+\epsilon_2}) = (0.5705, 0.1708), \tag{7}$$

so that Z is a facultative omnivore if

$$0 < \sigma_Z < \sigma_{Zmin} = 0.1708, \tag{8}$$

and an obligate omnivore, (requiring the presence of P_1 to survive) if:

$$0.1708 < \sigma_Z < \sigma_{Zmax} = 0.5705. \tag{9}$$

If $\sigma_Z > 0.5705$, Z is no longer a viable population and dies out.

We shall therefore describe the dynamics in terms of bifurcation transition diagrams as σ_Z varies, for both $\rho = 0$ and $\rho = 1$.

2.2 Critical Points

Our analysis of the critical (or equilibrium) points of (1)-(4) and their linear stabilities uses the same notation and labelling as [5]. Indeed the analyses for the origin and prey-only critical points are identical to that in [5]. Also, there is no predator-only critical point nor a pure prey-prey critical point for $\sigma_Z > 0$.

Critical Point	Label (P_1, P_2, Z, N)
Origin	$(0, 0, 0, 1)$
Prey A	$(P_{1A}, 0, 0, N_A)$
Prey C	$(0, P_{2C}, 0, N_C)$
Predator-Prey D	$(P_{1D}, 0, Z_D, N_D)$
Predator-Prey F	$(0, P_{2F}, Z_F, N_F)$
Predator-Prey-Prey E	$(P_{1E}, P_{2E}, Z_E, N_E)$

Table 2. Critical Points of eqns (1)-(3), and their labels as in [5].

3 Generalist Predation $\rho = 1$, Indiscriminate Grazing

When $\rho = 1$, we have generalist predation. By evaluating the Jacobian of the rhs of equations (1)-(3) at each of the critical points listed in Table 2, we determined the eigenvalues and so the linear stability of each critical point

in terms of the predator mortality σ_Z. We then combined these results with numerical integrations of equations (1)-(3) to produce a bifurcation transition diagram in terms of the maximum and minimum values of prey P_2 as σ_Z varies.

To produce the transition diagram, we fixed σ_Z and integrated the system numerically for $20,000$ time units, ignoring transients. We plotted the maximum and minimum values of prey P_2 over each oscillation; for steady states, these reduce to the steady state value of P_2 for the relevant critical point. We then took the final variable values as the initial conditions for the next value of σ_Z and repeated the procedure. The results are summarised in Fig. 1.

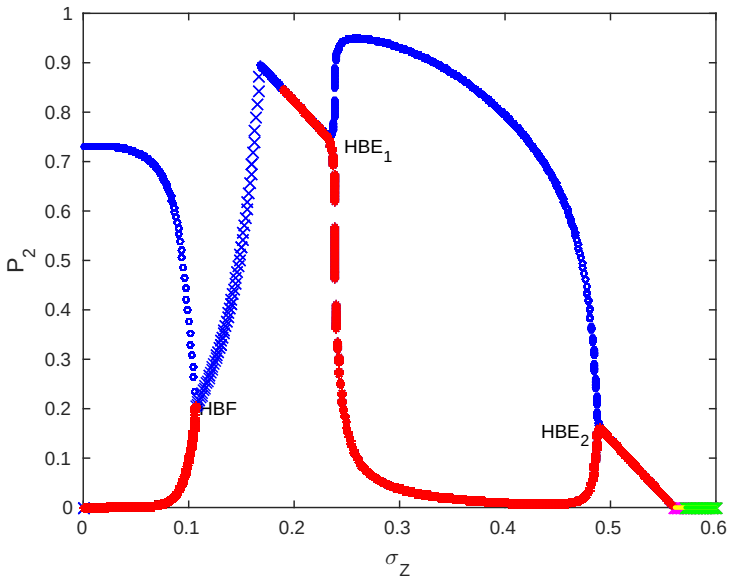

Fig. 1. Bifurcation transition diagram for generalist grazing ($\rho = 1$) for $0 \leq \sigma_Z \leq 0.6$.'Blue o' indicate maximum and 'red *' minimum values of the amplitude of P_2 over each cycle. The 'x' denotes the stable critical point F steady state, the yellow denotes the stable critical point D steady state, and the green the stable critical point A state. HBn denotes Hopf bifurcation for critical point n. There are two branches of stable critical point E steady states, one joining the end of the steady critical point F steady state to HBE_1, the other joining HBE_2 to the stable critical point D steady state.

For $0 < \sigma_Z < 0.11$, we obtain stable (P_2, Z, N) limit cycle oscillations. This predator-prey state then undergoes a supercritical Hopf Bifurcation at $\sigma_Z = 0.11$ (labelled as HBF in Fig. 1), following which we have stable critical point $(0, P_{2F}, Z_F, N_F)$ steady states for $0.11 < \sigma_Z < 0.17$. $(0, P_{2F}, Z_F, N_F)$ then loses stability to stable critical point $(P_{1E}, P_{2E}, Z_E, N_E)$ steady states, which exist in the region $0.17 < \sigma_Z < 0.225$. Stable (P_1, P_2, Z, N) oscillations then appear via a supercritical Hopf bifurcation (labelled as HBE_1 in Fig. 1). These oscillations persist until a second supercritical Hopf bifurcation (HBE_2)

at $\sigma_Z = 0.49$ gives rise once more to stable $(P_{1E}, P_{2E}, Z_E, N_E)$ steady states for $0.49 < \sigma_Z < 0.56$, before $P_2 \to 0$ and this prey-prey-predator state loses stability to a stable $(P_{1D}, 0, Z_D, N_D)$ steady state at $\sigma_Z = 0.56$. This critical point D steady state has a very small window of stability: $0.56 < \sigma_Z < 0.57$. For $\sigma_Z > 0.57$, Z is no longer viable as $Z \to 0$ and we are left with only a stable A prey steady state thereafter.

We found no evidence of chaotic states for $\rho = 1$.

Fig. 2 shows the time series and phase portrait for the facultative omnivore (P_2, Z, N) when $\sigma_Z = 0.05$. The time scale is such that 3650 time units ≈ 1 year. Fig. 3 shows time series and a three-dimensional phase portrait for the

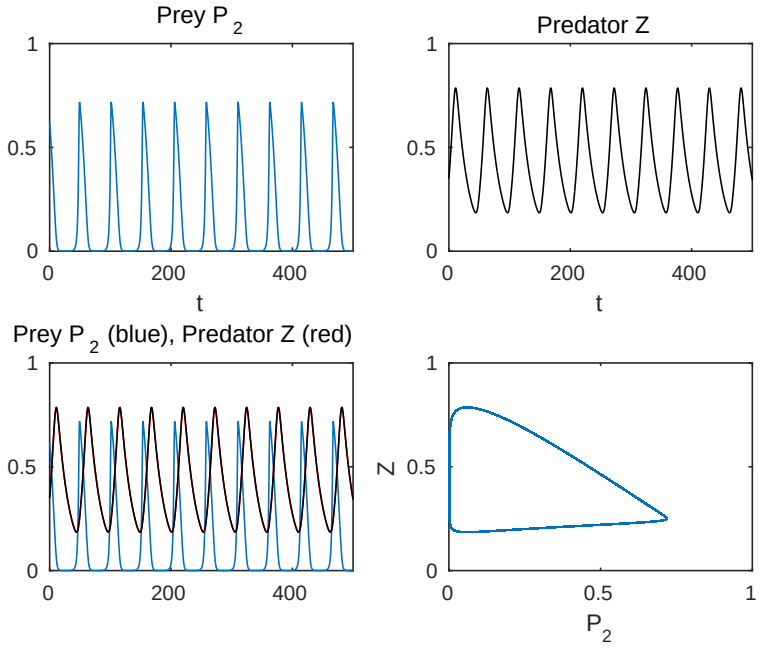

Fig. 2. P_2 and Z time series, and the (P_2, Z) phase portrait for the facultative omnivore predator-prey F for $\rho = 1$ and $\sigma_Z = 0.05$.

obligate omnivore (P_1, P_2, Z, N) for $\sigma_Z = 0.45$.

4 Specialist Predation ($\rho = 0$, Discriminate Grazing)

When $\rho = 0$, we have specialist predation. Following the procedure outlined in the previous section, we produced a bifurcation transition diagram in terms of the maximum and minimum values of prey P_2 as σ_Z varies. The results are summarised in Fig. 4.

For $0 \leq \sigma_Z < 0.11$, we again obtain stable (P_2, Z, N) limit cycle oscillations. This F predator-prey state then undergoes a supercritical Hopf Bifurcation

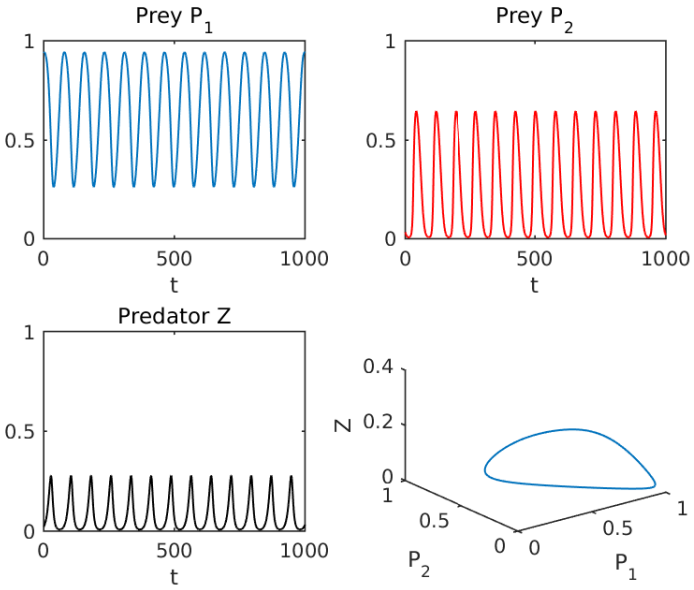

Fig. 3. P_1, P_2 and Z time series, and a 3-D phase portrait for the obligate omnivore $\rho = 1$ and $\sigma_Z = 0.45$.

(labelled as HBF in Fig. 4) at $\sigma_Z = 0.11$, following which we have a stable F steady state for $0.11 < \sigma_Z < 0.17$. $(0, P_{2F}, Z_F, N_F)$ then loses stability to $(P_{1E}, P_{2E}, Z_E, N_E)$ oscillations at $\sigma_Z \approx 0.168$. In view of (8), Z is a facultative omnivore in this region.

For $0.168 < \sigma_Z < 0.533$, P_1 is no longer zero and we find predominantly chaotic (P_1, P_2, Z, N) oscillations, before $P_2 \to 0$, resulting in this prey-prey-predator state losing stability to a stable (P_{1D}, Z_D, N_D) steady state at $\sigma_Z = 0.533$. This critical point D steady state is stable in a larger window of $0.533 < \sigma_Z < 0.57$ than for the generalist case. From (9), Z is now an obligate omnivore, requiring the presence of P_1 to exist.

The prey-only critical point A is unstable for $\sigma_Z < 0.57$. For $\sigma_Z > 0.57$, Z is no longer viable as $Z \to 0$ and we are left with only a stable critical point prey A steady state thereafter.

We now show plots of time series and phase portraits for selected values of σ_Z in the range $0.17 < \sigma_Z < 0.53$, chosen from Fig. 4.

For $\sigma_Z = 0.2$, we are just inside the chaotic regime for the obligate omnivore (P_1, P_2, Z, N). Since Z requires the presence of P_1 to exist, Fig. 5 shows that P_1 and Z are synchronised, with Z leading P_1, but both are out of phase with P_2. The (P_1, P_2, Z) phase portrait shows that the system never visits the interior of the (P_1, P_2) plane, in contrast to the example shown in Fig. 6.

When $\sigma_Z = 0.3$, we are in the middle of the chaotic regime for E. Fig. 6 shows P_1 and Z are still synchronised, with $min(Z) \approx 8.10^{-15}$, but out of phase with P_2. Now the trajectory visits the interior of the (P_1, P_2) plane.

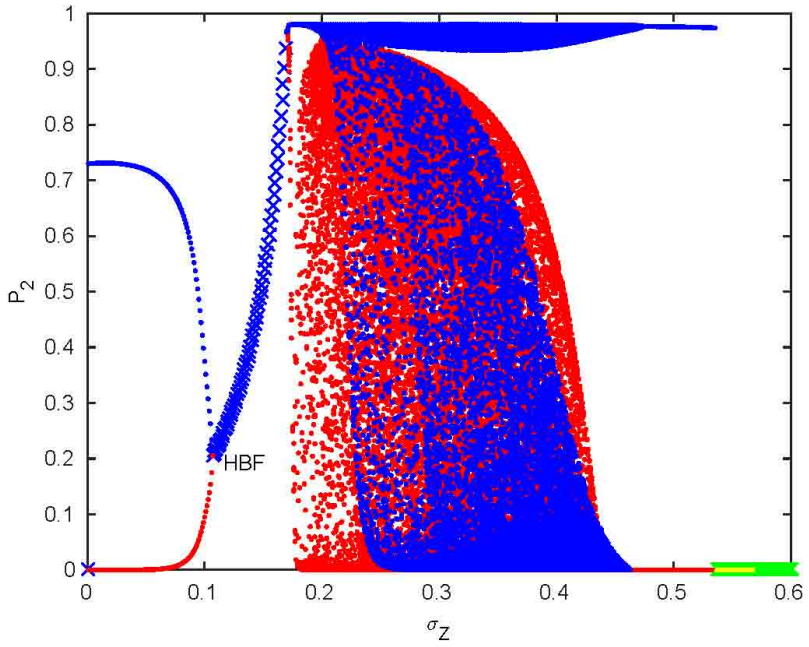

Fig. 4. Bifurcation transition diagram for specialist grazing ($\rho = 0$) for $0 \leq \sigma_Z \leq 0.6$, showing the maximum (blue 'o') and minimum (red '*') values of the amplitude of P_2 over each cycle as σ_Z varies. Also shown are regions of stability of critical point F steady states (blue 'x'), critical point D steady states (yellow $'o'$) and critical point A steady states (green $'o'$). HBF denotes the supercritical Hopf Bifurcation for critical point F.

Intermingled with the chaotic behaviour, there are small windows of periodicity. Fig. 7 shows the behaviour in one such window (which extends from $0.329 < \sigma_Z < 0.331$) for $\sigma_Z = 0.33$. Fig. 8 shows chaotic 'pinball' dynamics: P_1 and P_2 alternate in dominance; Z is still linked with P_1. Rapid oscillations in P_1 and Z are interleaved with long slow oscillations, each irregular. In comparison with Figs. 5 and 6, counter-intuitively, an increase in Z mortality σ_Z, has rendered Z more robust. Again note the trajectories do not visit the interior of the (P_1, P_2) plane.

Just prior to loss of stability of the E state, Fig. 9 shows a periodic (P_1, P_2, Z, N) cycle. Here $min(P_2) \approx 6.10^{-42}$. Since $20,000$ time units ≈ 6 years, the very low values for P_2 between sudden growth spurts, could be misconstrued as possible extinction of P_2. This is an example of a 'breather': in dynamical systems language, this is where a solution arises out of exponentially small terms.

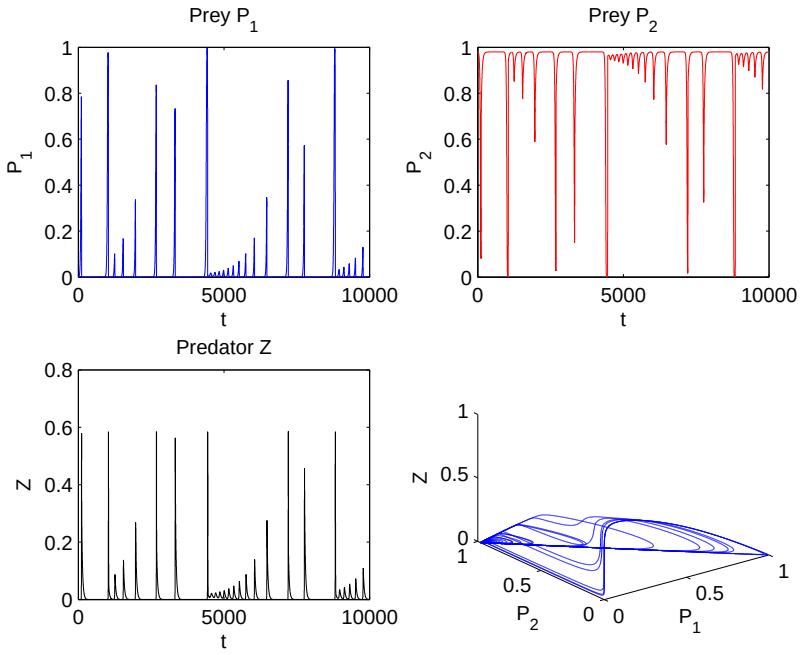

Fig. 5. Time series for P_1, P_2 and Z, and a 3-D (P_1, P_2, Z) phase portrait for $\rho = 0$ and $\sigma_Z = 0.2$.

5 Discussion

In this paper we reported on our investigations of a system of four coupled nonlinear ordinary differential equations for plankton predator-prey-prey interactions, comprising two phytoplankton P_1, P_2 populations, one zooplankton Z population, and one limiting nutrient N. Because of the constraint $P_1 + P_2 + Z + N = 1$, this system reduces to three coupled nonlinear differential equations for P_1, P_2, Z.

We considered four different types of grazing using measured parameter values:

- specialist (or discriminate) and facultative: $\rho = 0$, $0 < \sigma_Z < 0.1708$;
- specialist and obligate (Z requires the presence of P_1 to exist): $\rho = 0$, $0.1708 < \sigma_Z < 0.5705$;
- generalist (or indiscriminate) and facultative: $\rho = 1$, $0 < \sigma_Z < 0.1708$;
- generalist and obligate: $\rho = 1$, $0.1708 < \sigma_Z < 0.5705$.

These different grazing strategies create very different system behaviours. For specialist grazing, the system exhibits periodic (P_2, Z, N) limit cycle behaviour as well as stable critical point F steady states for $\sigma_Z < 0.1708$, before losing stability to chaotic (P_1, P_2, Z, N) behaviour, interspersed with thin periodic windows. Numerical integrations show long periods when P_2 takes very small

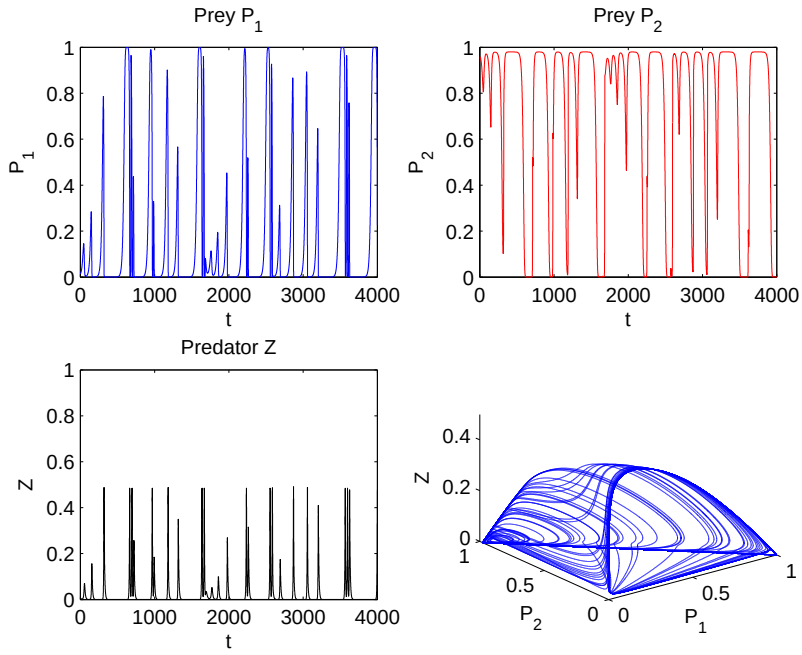

Fig. 6. As in Fig. 5 but for $\sigma_Z = 0.3$.

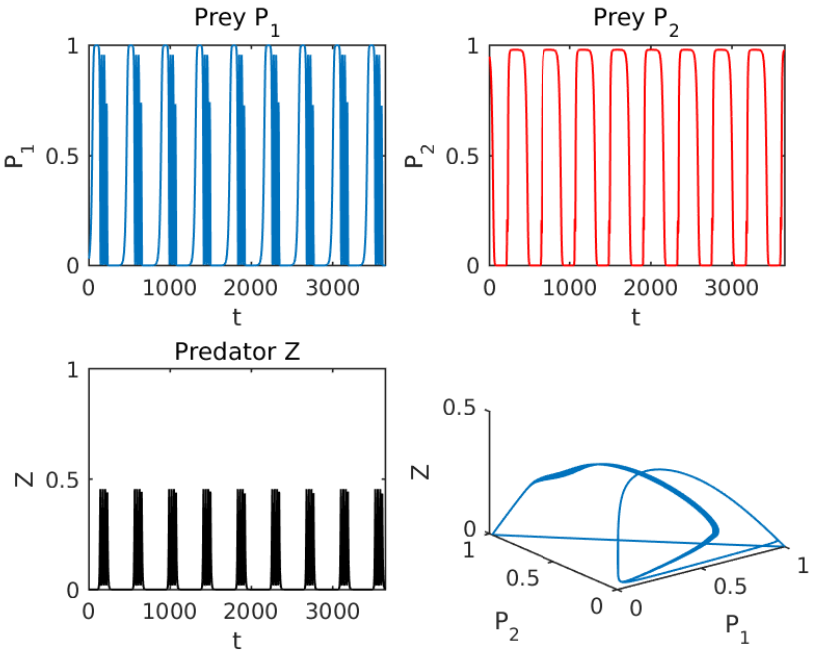

Fig. 7. Periodic E solutions for $\rho = 0$ and $\sigma_Z = 0.33$.

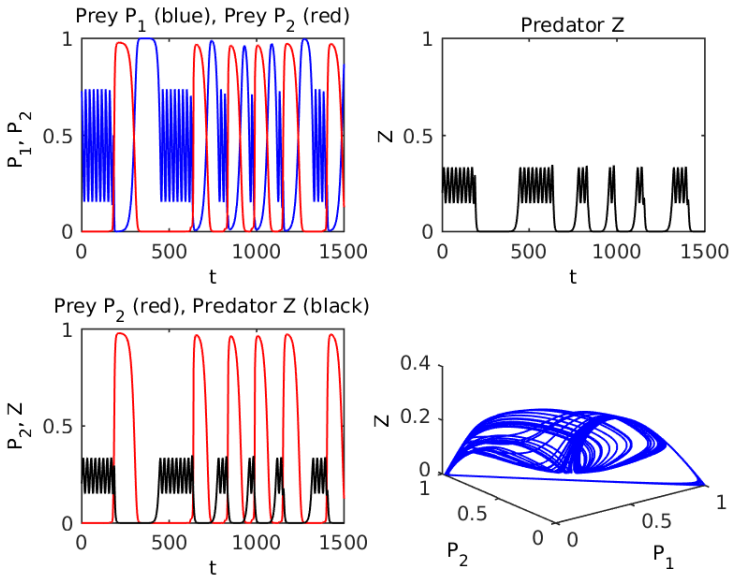

Fig. 8. Chaotic 'pinball' dynamics: rapid oscillations, with long slow oscillations, interspersed for $\rho = 0$ and $\sigma_Z = 0.45$.

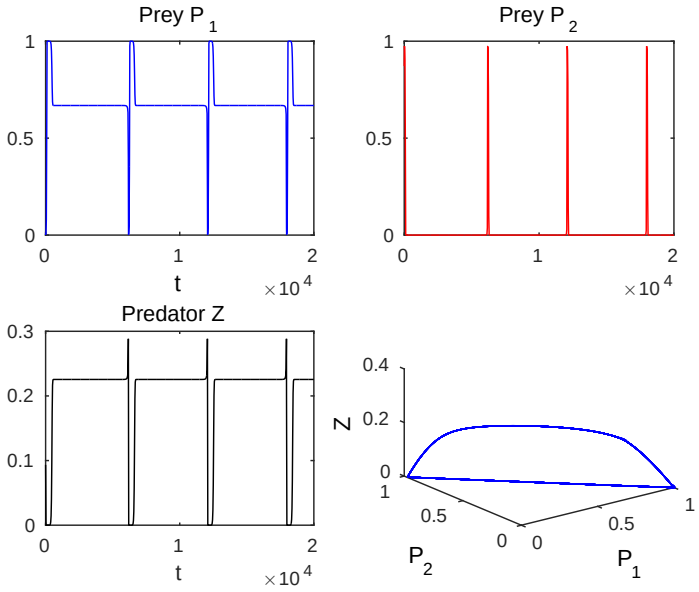

Fig. 9. Long periodic oscillations of E for $\rho = 0$ and $\sigma_Z = 0.53$.

values, but then recovers. Such behaviour could have significant implications in both climate change studies and fisheries management.

For generalist grazing, the model exhibits only simple oscillations or stable steady states, regardless of Z being a facultative or an obligate omnivore.

Less complex than operational models such as PlankTOM5 [13] or PlankTOM10 [12], our model has interesting and complicated limit cycle behaviour for measured parameter values that correspond to plankton blooms in the Earth's oceans. For operational models, obligate generalist grazers appear to provide the most desirable outcomes of stability and predictability, thereby giving more reproducible results under changes in environmental forcings.

References

1. T.R. Anderson, W. Gentleman, B. Sinha. Influence of grazing formulations on the emergent properties of a complex ecosystem model in a global ocean general circulation model. *Progress in Oceanography* 87, 201–213, 2010.
2. G. Billen and S. Becquevort. Phytoplankton: bacteria relationships in the Antarctic marine ecosystem. *Pol.Res*, 10, 245–253, 1991.
3. P. Bork, C. Bowler, C. de Vargas, G. Gorsky, E. Karsenti, and P. Wincker. Tara Oceans studies plankton at planetary scale. *Science*, 348, 873, 2015.
4. R.J. Charlson, J.E. Lovelock, M.O. Andreae and S.G. Warren. Oceanic phytoplankton, atmospheric sulphur, cloud albedo and climate. *Nature*, 326, 655–661, 1987.
5. R. A. Cropp and J. Norbury. Parameterizing plankton functional type models: insights from a dynamical systems perspective. *Journal of Plankton Research*, 31, 939–963, 2009.
6. R. A. Cropp, I.M. Moroz and J.Norbury. The role of grazer predation choices in the dynamics of consumer-resource based ecologies. Submitted, 2015.
7. P. Falkowski. The power of plankton. *Nature*, 483, 817–820, 2012.
8. T. Fenchel. Ecology of heterotrophic microflagellates. IV. Quantitative occurrence and importance as bacterial consumers. *Mar. Ecol. Progress Ser.*, 9, 35–42, 1982.
9. A.J. Gabric, P.A. Matrai and M. Vernet. Modelling the production and cycling of dimethylsulphide during the vernal bloom in the Barents Sea. *Tellus*, 51B, 919–937, 1999.
10. A.J. Gabric, P.H. Whetton and R.A. Cropp. Dimethylsulphide production in the sub-Antarctic southern ocean under enhanced greenhouse conditions. *Tellus*, 53, 273–287, 2001.
11. B. Hansen, S. Christiansen and G. Pedersen. Plankton dynamics in the marginal ice zone of the central Barents Sea during spring: carbon flow and the structure of the grazer food chain. *Polar Biol.*, 16, 115–128, 1996.
12. L. Kwiatkowski, A. Yool, J.I. Allen, T.R. Anderson, R. Barciela, E.T. Buitenhuis, M. Butenschn, C. Enright, P.R. Halloran, C. Le Quéré, L. de Mora, M.F. Racault, B. Sinha, I.J. Totterdell, and P.M. Cox. iMarNet: an ocean biogeochemistry model intercomparison project within a common physical ocean modelling framework. *Biogeosciences*, 11, 7291–7304, 2014.
13. C. Le Quéré, S.P. Harrison, I.C. Prentice, E.T. Buitenhuis, O. Aumont, L. Bopp, H. Claustre, L.C. Da Cunha, R. Geider, X. Giraud, C. Klaas, K.E. Kohfeld, L. Legendre, M. Manizza, T. Platt, R.B. Rivkin, S. Sathyendranath, J. Uitz, A.J. Watson and D. Wolf-Gladrow. Ecosystem dynamics based on plankton functional types for global ocean biogeochemistry models. *Global Change Biology*, 11, 2016–2040, 2005.

14. C.L. Moloney, M.O. Bergh, J.G. Field and R.C. Newell. The effect of sedimentation and microbial nitrogen regeneration in a plankton community: a simulation investigation. *J. Plankton Res.*, 8, 427–445, 1986.
15. G. Muller-Niklas and G.J. Herndl. Dynamics of bacterio-plankton during a phytoplankton bloom in the high Arctic waters of the Franz-Joseph Land archipelago. *Aquat. Microb. Ecol.*, 11, 111–118, 1996.
16. S.F. Sailley, M. Vogt, S.C. Doney, M.N. Aita, L. Bopp, E.T. Buitenhuis, T. Hashioka, I. Lima, C. Le Quéré and Y. Yamanaka. Comparing food web structures and dynamics across a suite of global marine ecosystem models. *Ecological Modelling*, 261 262, 43–57, 2013.
17. D. Slagstad and K. Stole-Hansen. Dynamics of plankton growth in the Barents Sea. *Polar Res.*, 10, 173–186, 1991.